

POLYMER PROCESS ENGINEERING

Eric A. Grulke



P T R. Prentice Hall
Englewood Cliffs, New Jersey 07632

Library of Congress Cataloging in Publication Data

Grafke, Eric A.
Polymer process engineering / by Eric A. Grafke.
p. cm.
Includes index.
ISBN 0-13-015397-4
1. Polymers. I. Title.
TP267.G78 1994
665.2—dc20

93-22178
C3P

Editorial/production supervision and interior design: Northeastern Graphic Services, Inc.
Cover design: Lustigman Graphics
Buyer: Mary Elizabeth McCartney
Acquisitions editor: Betty Sun



©1994 by PTR Prentice Hall
Prentice-Hall, Inc.
A Paramount Communications Company
Englewood Cliffs, New Jersey 07632

The publisher offers discounts on this book when ordered in bulk quantities. For more information, contact:

Corporate Sales Department
PTR Prentice Hall
113 Sylvan Avenue
Englewood Cliffs, NJ 07632

Phone: 201-392-2883
Fax: 201-292-2249

All rights reserved. No part of this book may be reproduced in any form or by any means, without permission in writing from the publisher.

Printed in the United States of America
10 9 8 7 6 5 4 3 2 1

ISBN 0-13-015397-4

Prentice-Hall International (UK) Limited, London
Prentice-Hall of Australia Pty. Limited, Sydney
Prentice-Hall Canada Inc., Toronto
Prentice-Hall Hispanoamericana, S.A., Mexico
Prentice-Hall of India Private Limited, New Delhi
Prentice-Hall of Japan, Inc., Tokyo
Simon & Schuster Asia Pte. Ltd., Singapore
Editor: Prentice-Hall do Brasil, Ltda., Rio de Janeiro

Contents

Preface xiii

Trademarks xv

Chapter 1 A Primer of Polymer Science and Engineering 1

1.1 GENERAL TYPES OF POLYMERS 1

1.2 POLYMER PRODUCTS AND INDUSTRIES 7

1.2.1 Plastics 8

1.2.2 Elastomers 11

1.2.3 Fibers 13

1.2.4 Coatings 16

1.2.5 Adhesives 16

1.2.6 Foams 17

1.2.7 Composites and Fiber-Reinforced Materials 17

1.3 POLYMER NOMENCLATURE 18

1.3.1 Rules 19

1.4 CONSEQUENCES OF LONG CHAIN LENGTH 20

1.5 CHEMICAL BONDING IN POLYMERS 22

1.5.1 Types of Primary Bonds 22

1.5.2 Secondary Bonding Forces 23

1.6 MOLECULAR WEIGHT AND MOLECULAR WEIGHT DISTRIBUTION 26

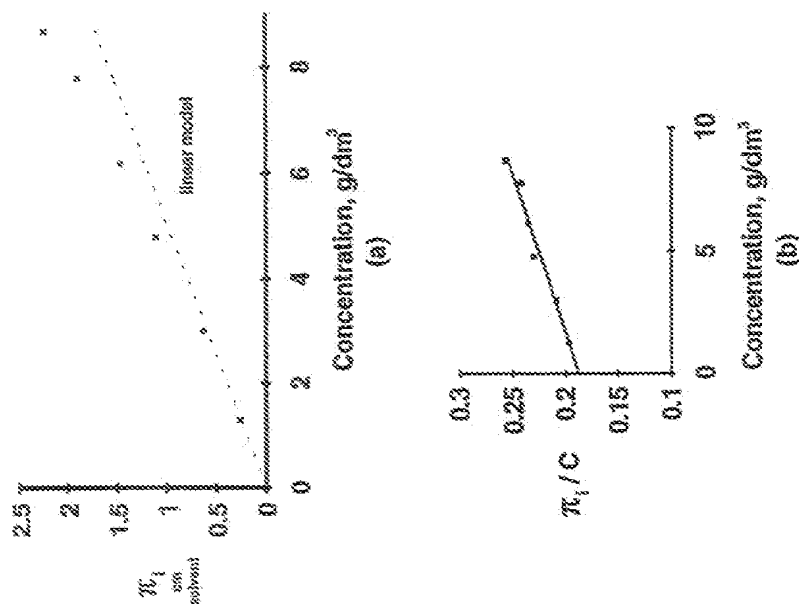


Figure 6.3 Osmotic pressure data. Polystyrene in methyl ethyl ketone. Data from Table 6.6 (a) π_i/c ; (b) π_i/c vs. c .

molecular weight is the Stokes-Einstein equation, which relates the relative viscosity of a dispersion of spherical particles to their volume fraction as the dispersed phase.

Table 6.7 shows some definitions of different viscosities. One of the more commonly reported measurements is that of intrinsic viscosity, which is independent of concentration (actually the limiting value for inherent viscosity as polymer concentration goes to zero). Intrinsic viscosity is affected by the choice of solvent. An important correlating tool is the Mark-Houwink relationship.

$$[\eta] = K M^a$$

6.43

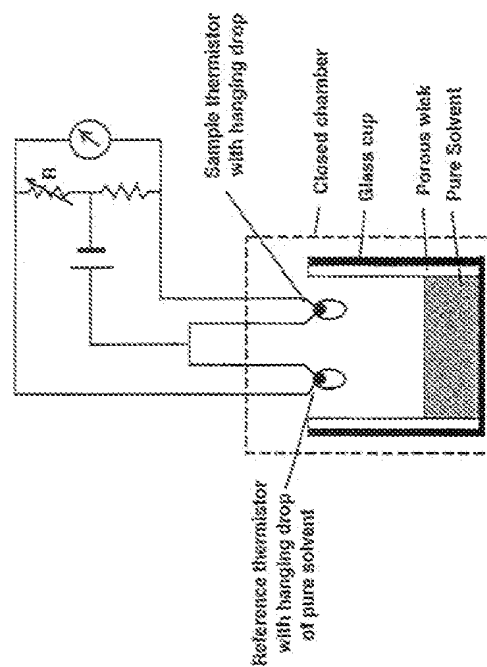


Figure 6.10 Schematic diagram of vapor point depression equipment.

where $[\eta]$ is the intrinsic viscosity, K is a constant, and a is the power exponent on molecular weight. The power exponent a , typically has values in the range of 3.4 for high polymers, and much theoretical effort has been expended to predict the value of a from first principles. The constants for Equation 6.43 change depending on the polymer-solvent system considered and should be obtained for each case. Table 1 in Appendix F contains a table of Mark-Houwink parameters for several solvent systems. The average molecular weight obtained by viscosity

TABLE 6.7 Definitions of Different Viscosity Types

Symbol	Type of Viscosity	Equation	Units	IUPAC
η	Solution	---	Poise	
η_0	Solvent	---	Poise	
η_r	Relative	η/η_0	Dimensionless	Viscosity ratio
η_{sp}	Specific	$\left(\frac{\eta - \eta_0}{\eta_0} \right) / c$	Dimensionless	
η_{in}	Inherent	$(\ln \eta_r)/c$	Deciliter/g	
$[\eta]$	Intrinsic	$(\eta_{sp}/c)_{c \rightarrow 0} \propto (\ln \eta_r)/c_{c \rightarrow 0}$	Deciliter/g	Limiting viscosity number
η_{red}	Reduced	η_{sp}/c	Deciliter/g	

and constant velocity. The integral and several of the parameters are constant for a specific viscometer, so the flow time is

$$t = \frac{\eta}{Ap} \quad 6.45$$

where A is the viscometer constant. The quantity, η/p , is the dynamic viscosity of the fluid. The viscometer constant is determined by calibrating it with standard solutions.

The ratio of the solution viscosity to the solvent viscosity is the reduced viscosity,

$$\eta_r = \frac{\eta}{\eta_0} = \frac{t_p}{t_0} \quad 6.46$$

where η_0 is the reduced viscosity and the c subscripts refer to solvent values. The density ratio is often one for dilute solutions so that the reduced viscosity is the ratio of flow times. The reduced viscosity approaches one as a limit when the polymer concentration approaches zero. The specific viscosity describes the fractional increase in viscosity caused by the polymer,

$$\eta_{sp} = \eta_r - 1 = \frac{t - t_0}{t_0} \quad 6.47$$

The specific viscosity is nonlinear with polymer concentration and has been modeled using a power series expansion.

$$\eta_{sp} = \frac{\eta_{sp}}{C} = [\eta] + \alpha C + \beta C^2 + \dots \quad 6.48$$

The reduced viscosity, η_{sp}/c , is the ratio of the specific viscosity to the concentration. It has a limiting value as concentration approaches zero of $[\eta]$, the intrinsic viscosity. The intrinsic viscosity is a measure of the polymer's ability to increase solution viscosity in the absence of intermolecular effects (in the limit as C goes to zero).

It has been difficult to relate the coefficients α and β of Equation 6.48 to the properties of the polymer solution. There are two popular empirical models for solution viscosities. The Huggins model assumes that the α coefficient is proportional to $[\eta]^2$.

$$\frac{\eta_{sp}}{C} = [\eta] + k[\eta]^2 C \quad 6.49$$

A plot of η_{sp}/c versus C should be linear with an intercept of $[\eta]$ and a slope of $k[\eta]^2$. The Huggins coefficient, k , usually is a constant for polymer solvent and often has a value between 0.3 and 0.5.

measurements lies between the number and weight average molecular weights. Experimental results give the exponent for the Moynihan relation (Eq. 6.11) between $0.5 < c < 0.8$.

Capillary viscometers are easy to use and are often used in polymer laboratory experiments. Figure 6.11 shows several types of these devices. The measurement is based on the laminar flow of polymer solution through a tube of constant radius. Polymer solution is drawn into the reservoir above the capillary tube (on the right-hand side of each device) and the flow is started. The time for the solution meniscus to pass from the upper reservoir mark to the lower reservoir mark is measured. The time required for the process to occur is

$$t = \frac{8\eta L}{\pi g \rho R^4} \int_{h_1}^{h_2} \frac{dh}{h} \quad 6.44$$

where L is the capillary length, R is the radius, t_1 and t_2 are the upper and lower liquid head heights, Q is the volumetric flow of solution, ρ is the density, and η is the solution viscosity. Equation 6.44 is derived by solving the equation of motion for constant flow

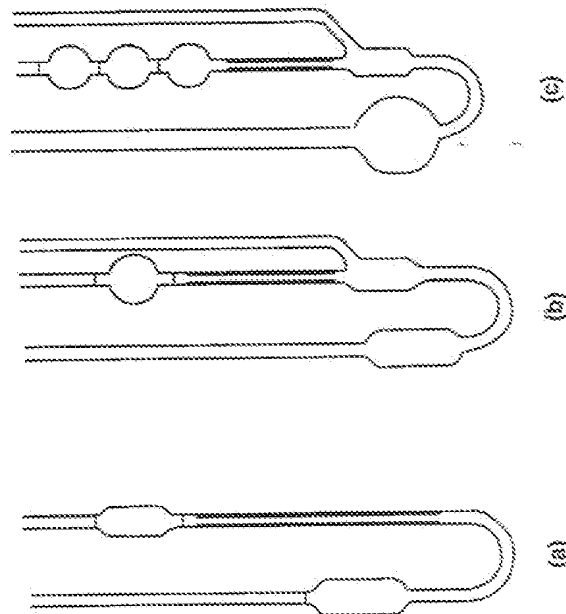


Figure 6.11 Several types of capillary viscometers.

The inherent viscosity, in η/c , often approaches a limiting value as concentration goes to zero. The Kraemer model uses this property to estimate $[\eta]$:

$$\ln \eta_{sp} = \frac{\eta_{sp}}{C} = [\eta] + k'[\eta]^2 C \quad (6.30)$$

EXAMPLE 6.6 INTRINSIC VISCOSITY OF POLYMETHYL METHACRYLATE IN CHLOROFORM AT 35°C.

A student has taken some capillary rheology data and needs to determine the intrinsic viscosity of the sample. The data are shown in the following table.

Concentration, g polystyrene/cm ³	Flow Time, s
0 (pure solvent)	25
.0015	51.1
.0033	39.6
.0047	47.2
.0062	56.1
.0095	79.1

This problem can be solved by using Equations 6.46 and 6.47 to calculate η_{sp} plotting η_{sp}/C versus C and then determining the slope and intercept. The conversion of the raw data is shown in Table 6.8. Figure 6.12 shows the data plotted using Equation 6.48. The solid curve is the Huggins model using $[\eta] = 132$ and $k = 0.35$. The model fits this data set well.

Both models are plotted on the same graph to give a value for the intrinsic viscosity. There are alternative models for determining the intrinsic viscosity from capillary rheometer measurements. Table 6.9 lists some of them.

Relation between Intrinsic Viscosity and Molecular Size. The intrinsic viscosity has importance beyond simple viscosity measurements. It can be related to the size of the polymer molecule in solution as well as to its molecular weight. Table 6.10 gives some of these methods. The Einstein-Simha model is based on the viscosity of a solution of large particles. Its application depends on defining V_0 , the hydrodynamic volume.

The Flory-Fox model is based on the partially permeable polymer coil model. It leads to an equation relating the intrinsic viscosity to the radius of the polymer in solution and the molecular weight. However, the polymer radius is a function of a molecular weight, so the result is

Sec. 6.4 Measurement of Molecular Weight

TABLE 6.8 Conversion of Flow Data to η_{sp}/C

C , g/cm ³	t , s	η_t	η_{sp}	η_{sp}/C , cm ² /g
0	25	1	—	—
.0015	51.1	1.244	.244	163
.0033	39.6	1.584	.584	177
.0047	47.2	1.888	.888	189
.0062	56.1	2.244	1.244	201
.0095	79.1	3.164	2.164	228

$$[\eta] = \phi_p \left(\frac{\langle r^2 \rangle_0}{M} \right)^{3/2} \propto M^{1/2} \quad (6.51)$$

where ϕ_p is a constant (2.5×10^{21} for many flexible polymers in good solvents).

6.4.5 Gel Permeation Chromatography

GPC measurements have become popular recently because they yield continuous distributions and can be automated. They are based on the mechanical separation effected by flowing a pulse of polymer solution through a packed bed of porous particles. At slow flow rates, small molecules will diffuse into the pores of the bed and their net velocity through the bed will be retarded. Large particles will not diffuse as quickly and will flow through the interstitial space (Fig. 6.13). An absorbance detector monitors the effluent stream to detect polymer concentration as a function of time. GPC curves have the large polymer molecules exiting

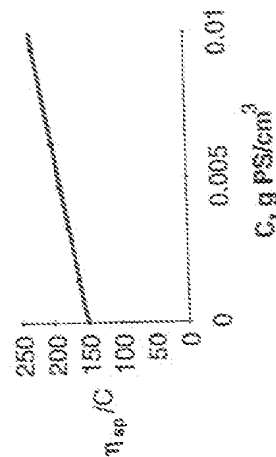


Figure 6.12 Plot of reduced viscosity versus concentration. Polymethyl methacrylate in chloroform at 35°C.